Dalton Transactions

Accepted Manuscript

ROYAL SOCIETY OF CHEMISTRY

www.rsc.org/dalton

Crystal structure, DFT, spectroscopic and biological activity evaluation of analgin complexes with Co(II), Ni(II) and Cu(II)

Ahmed M. Mansour

Chemistry Department, Faculty of Science, Cairo University, Gamaa Street, Giza 12613, Egypt

Abstract

Reaction of analgin (NaL) with Co(II), Ni(II) and Cu(II) salts in ethanol affords complexes of the type $[ML_2]$, which were characterized by elemental analysis, FT IR, UV-Vis., EPR, TG/DTA, magnetic susceptibility and conductance measurements. The copper(II) complex crystallizes in the orthorhombic *Pbca* space group. Analgin behaves as a mono-negatively tridentate ligand *via* pyrazolone O, sulfonate O and tertiary amino group. The interaction of the tertiary nitrogen with M^{n+} ions is the main factor, which determines the stability of complexes as revealed from natural bond orbital analysis data, where the binding energy decreases with an increase in the bond length of M-N bond. Time-dependent density functional theory calculations were applied in order to realize the electronic structures and to explain the related experimental observations. The anti-bacterial activity was studied on *Staphylococcus aureus* and *Escherichia coli*. Coordination of analgin to Ni(II) and Cu(II) leads to a significant increase in its antibacterial activity compared with the Co(II) complex.

Key Words: Dipyrone; Crystal structure; NBO; Biological activity

* Corresponding author, Tel.: +2 02 01222211253; Fax: +20 2 35728843. E-mail: inorganic_am@ yahoo.com

Introduction

Analgin (dipyrone, metamizole or novalgin) (Scheme 1) is the sodium salt of [(1,5-dimethyl-3-oxo-2-phenylpyrazol-4-yl)-methylamino]methansulfonate. This drug presents antipyretic and analgesic activity **[1]** as well as other beneficial effects such as vascular smooth muscle relaxant, anti-apoptotic, and anti-convulsant **[2]**. Analgin has both spasmolytic action and analgesic effect makes it a favorable drug for colic pain **[3]**. However, the administration of analgin may be associated with severe effects as chemical intolerance and agranulocytosis **[4]**. The mode of action involves the hydrolysis to 4-methyl-aminoantipyrine, with the latter further converted to other metabolites by various enzymatic reactions **[5]**. Analgin forms the active constituent of several drugs and as a binary mixture with acetylsalicyclic acid, and paracetamol. Several analytical techniques such as UV-Vis. **[6]**, fluorescence **[7]**, HPLC **[8]**, flow injection analysis **[9]**, and polarographic **[10]** were applied for the determination of analgin in the pharmaceuticals.

So far, pyrazolone and its derivatives were acknowledged to possess a wide range of industrial and pharmaceutical applications, which attracted considerable scientific and applied interest **[11-12]**. Thus, it was essential for the inorganic chemists to shed more light about the coordination behavior of analgin. To best of knowledge, no X-ray crystal data for metal complexes of analgin was reported in the literature makes the structures of these compounds ambiguous. Binary complexes of the type ML_2 (M = Co^{II}, Ni^{II}, Cu^{II}, and Zn^{II}) and $Cd(NaL)_2Cl_2$ were reported in the literature by Tatwawadi **[13]**, who assumed the interaction of analgin with M^{n+} as a bidenate ligand. Several mixed-ligand complexes of VO^{2+}, Cr^{III}, Mn^{II}, Co^{III}, Ni^{II}, Mo^{II}, WO_2^{VI}, and Hg^{II} metal ions were also synthesized and characterized by Maurya *et al.* **[14]** supposing analgin coordinated through only the pyrazolone O atom. Besides, the reaction between analgin and Fe^{III} in presence of different anions was followed by means of UV, IR, and pH-metric titrations **[15]**. The composition and stability of Hg^{II} complexes were pH-metrically studied **[16]**, where the development of complexes assumed to proceed through only the pyrazole ring O and SO_3 group.

The search for the new effective antimicrobial agents is of paramount importance, but the discovery of new drugs having completely new chemical structures is time consuming and expensive. Thus, molecular structure modification is better and desirable. Analgin presents a chemical structure that favors chemical modifications by means of complexation with some transition metal ions. In the present study, Co(II), Ni(II) and Cu(II) complexes of analgin antipyretic drug were synthesized, and characterized, and tested for their biological activity against *Staphylococcus aureus*, and *Escherichia coli*. Structural properties have been studied both experimentally and theoretically and are correlated here. Natural bond orbital (NBO) analysis has been also performed to provide details about the type of hybridization, and the nature of bonding in the studied complexes. With the aim of under-standing the electronic structures of the complexes, and the related experimental observations, TD-DFT calculations were applied.

Results and discussion

Structural characterization

The reaction of $Co(NO_3)_2{\cdot}6H_2O$, $Ni(CH_3COO)_2{\cdot}4H_2O$, and $Cu(NO_3)_2{\cdot}3H_2O$ with two equivalent of analgin in ethanol affords pink (**1**), blue (**2**) and crystalline green (**3**) complexes of the type $[ML_2]$ in that order (Scheme 1). These complexes were characterized by elemental analysis, TG/DTA, IR, EPR, UV-Vis., magnetic and conductance measurements. However, unambiguous proof of the tridentate behavior of analgin *via* pyrazolone O, sulfonate O and tertiary amino group to the metal ions finally came from the single crystal X-ray analysis of complex **3**. Relevant parameters are listed in Table 1 and

the molecular structure of [CuL_2] is shown in Fig. 1. Among the various vibrational bands of analgin, the studies of the C=O, C-N, and SO_3 modes were found to be useful in determining the coordination sites. The FT IR spectrum of analgin showed strong stretching C=O band at 1660 cm^{-1}, which shifted to lower wave number, 1604 **(1)**, 1611 **(2)**, and 1600 **(3)** suggesting the participation of the C=O group in the coordination sphere of the metal ions. The assignment of the stretching bands of the C-N and SO_3 groups in the region between 1400 and 1000 cm^{-1} is not easily interpreted owing to their overlap with the aromatic bands. Therefore, it was necessary to compare first the spectrum of analgin with that of phenazole, which have a similar structure, but without the attached of $–N(CH_3)CH_2SO_3Na$ group to position 4 of the pyrazolone ring. In general, the non-coordinated anionic SO_3 shows two bands due to the asymmetric and symmetric stretching modes **[17]**. On coordination to the metal ion, three ν(SO) bands are observed as the C_{3v}-symmetry is broken. Comparison of analgin with phenazole showed two new bands at 1182 and 1051 cm^{-1} assigned to ν^{ss}(SO), while the asymmetric mode is overlapped. In complexes, the SO_3 group gave rise to doublet structure at (1265, 1166) (**1**), (1263, 1169) (**2**), and (1245, 1196 cm^{-1}) (**3**) corresponding to asymmetric and symmetric modes **[18]**. In addition, the ν^{ss}(SO) at 1051 cm^{-1} in analgin was shifted to 1019 (**1**), 1022 (**2**), and 1030 cm^{-1} (**3**) suggesting the contribution of SO_3 in the complex formation. The ν(C-N) in the uncoordinated analgin was found at 1343 cm^{-1}, and shifted to ≈ 1331 cm^{-1} in complexes. The most noteworthy observation is that the anion of the metal salt has no role in the complex formation as the IR spectra of the complexes, which were prepared from either the chloride or acetate salts are typical. Therefore, analgin behaves as a N,O,O tridentate ligand towards M^{n+} ions.

For complexes **1** and **3**, the thermal decompositions start from 270 and 236 ºC with a continuous weight loss in the temperature range of 270-546 and 236-561 ºC respectively. Three endothermic stages at 253, 383, and 513 ºC for **1**, and 220, 269, and 478 ºC for **3** were identified and assigned to organic ligand decomposition with high percentage of final residues (18.24% for **1** and 16.37% for **3**) at 1100 ºC. The final residue may be thought to be CoS_2 (calcd. 17.99 %; **1**), and carbonized CuS (calcd. 15.72 %; **3**) **[19]**. The simultaneous TG/DTA of **2** showed that the thermal decomposition takes place *via* three complicated stages maximized at 274, 411, and 475 ºC. These steps bring the total mass loss up to 88.73% of the parent complex. Such mass loss is close to the calculated value (89.08%) expected for the formation of NiO as a final residue.

Electronic structure, **magnetic, and EPR**

The crystal field theory of high spin octahedral Co(II) complexes **[20]** predicted three spin allowed

d-d transitions namely $^4T_{1g}\rightarrow{}^4T_{2g}(F)$ (ν_1), $^4T_{1g}\rightarrow{}^2A_{2g}$ (ν_2) and $^4T_{1g}\rightarrow{}^4T_{2g}(P)$ (ν_3). The electronic spectrum of **1** showed only one band in DMSO at 275 nm as well as a shoulder at 420 nm assigned to π-π^*/ aromatic system and n-π^*(C=O)/$^4T_{1g}\rightarrow{}^4T_{2g}(P)$ (ν_3), respectively. The effective magnetic moment (μ_{eff}) of 4.71 μ_B for complex **1** further complements the electronic spectral findings as this value lies in the acceptable experimental range (4.10-5.20 μ_B) for high spin cobalt(II) complexes **[21]**. The electronic ground state of octahedral Ni(II) complexes is $^3A_{2g}$ and three spin-allowed transitions; $^3A_{2g}\rightarrow{}^3T_{2g}$ (ν_1), $^3A_{2g}\rightarrow{}^3T_{1g}(F)$ (ν_2), and $^3A_{2g}\rightarrow{}^3T_{1g}(P)$ (ν_3) are expected **[22]**. Some octahedral Ni(II) complexes **[23]** showed a weak broad band at about 790 nm corresponding to the spin-forbidden $^3A_{2g}\rightarrow{}^1E_g$ transition. Complex **2** displayed three bands in DMSO at 275, 400 and 535 nm assigned to the internal ligand transitions, MLCT/n-π^* (C=O) and $^3A_{2g}\rightarrow{}^3T_{1g}$ (F) (ν_2), respectively, in an octahedral geometry. The μ_{eff} of **2** is found to be 3.70 μ_B (298 K) with presence of spin-orbital coupling **[24]**. This value exceeds the spin only value, but is not high as μ_{s+L} **[21]**. This happens because the electric fields of atoms, ions, and molecules surrounding metal ion in its compounds restrict the orbital motion of the electrons so that the orbital angular momentum and hence the orbital moments are partially quenched. For octahedral Cu(II) complexes, it has been established that the split of ^2E_g and $^2T_{2g}$ states of ^2D ground state may keep the three $^2B_{1g}\rightarrow{}^2A_{1g}$ (ν_1), $^2B_{1g}\rightarrow{}^2B_{2g}$ (ν_2) and $^2B_{1g}\rightarrow{}^2E_g$ (ν_3) electronic transitions unresolved in the spectra of the elongated tetragonal or rhombic distortions (D_{4h} symmetry) geometries. Complex **3** showed four bands in DMF at 270, 375, 485, and 780 nm. The broad band at 780 nm can be assigned in terms of overlapping of the ν_1-ν_3 bands in an octahedral geometry. The band at 485 nm has LMCT character, which may be originated from the SO_3 group, while those at 270 and 375 nm are attributed to π-π^*/ aromatic/n-π^*(C=O), respectively. The μ_{eff} of **3**, corrected for diamagnetic and temperature-independent paramagnetic contributions, is 2.57 μ_B (298 K). This value is higher than the spin-only value expected for non-interacting Cu^{II} ions (S = ½, $t_{2g}^6e_g^3$), but in the acceptable range for Cu(II) complexes **[21]**.

The X-band EPR spectrum of **3** in solid state (Fig. 2) at 298 K exhibits typical four lines noticeable $^{63/65}$Cu (I = 3/2) hyperfine splitting with $g_\parallel$ = 2.320 ($A_\parallel = 143\times10^{-4}$ cm^{-1}), and $g_\perp$ = 2.074 characterized of mononuclear copper(II) complexes having rhombic-octahedral with the elongation of the axial bonds or square-based pyramidal symmetries and $d_{x^2-y^2}$ orbital is the ground state. This spectrum usually obtains with large ligand like analgin that increase the Cu-Cu distance and decrease the line width **[25]**. The geometric parameter G, which is a measure of the exchange of interaction between the copper centers in a powdered sample, has been calculated **[26]** as $G = (g_\parallel - 2.0023)/(g_\perp - 2.0023)$. According to Hathaway **[27]** if G > 4, the exchange interaction is negligible and if G < 4, indicates

exchange interaction. The value of G is found to be 4.32 indicating absence of moderate exchange interaction among the copper molecules in the solid state.

Crystal structure

X-ray single-crystal diffraction data revealed that complex **3** crystallizes in the orthorhombic *Pbca* space group. A view of the molecular structure of **3** is shown in Fig. 1. Selected crystallographic data are presented in Table 2. The six-coordinated Cu(II) ion is arranged in a slightly distorted octahedral geometry, where two analgin molecules lying in a trans-conformation are acting as tridentate chelators forming four stable five-membered rings. An inversion centre of symmetry is found at the copper atom, where the two ligands are adjusted in a linear way, but pointing in opposite directions. The structure is coplanar, where the bond angles; O2-Cu-O2^{i}, N9-Cu-N9^{i}, and O13-Cu-O13^{i} equal 180 º. The coordination sphere consists of two pyrazolone oxygen atoms [CuO2 = 2.007(2) Å], two N [CuN9 = 2.009(2) Å] and two oxygen atoms [CuO13 = 2.321(2) Å] of SO_3 groups. The two anionic Cu-O13 bond lengths are equal, but they are longer than the Cu-O2 bond distances. As shown in Table 2, thedistortion around the copper atom is low, where the bond angles are significantly deviated from those of a regular octahedron. In the crystal packing, it is possible to observe π-π stacking interactions between the ring planes (Fig. 3a), and also the molecules are cross-linked to each other through O_2SO…H-C with a distance of 2.734 Å (Fig. 3b).

DFT/TD-DFT

To obtain an insight into the geometrical and electronic structure of the investigated complexes, [ML_2] (M = Co(II), Ni(II), and Cu(II)) were optimized (Fig. S1†) at DFT/B3LYP level of theory starting from the X-ray structure coordinates of the Cu(II) complex. The complexes were characterized as local minima through harmonic frequency analysis. Selected calculated bond lengths and angles are compared in Table S1†. A good agreement was found for the Cu-O bonds, while the value of the Cu-N bond is overestimated by the DFT method. The M-N bond distance increases from Ni to Co then Cu. The bond angles are slightly different by 2-3 º.This happens because the calculations were performed in gaseous state, whereas packing molecules with inter- and intra-molecular interactions are treated in the experimental measurements. The nature of the electronic transitions observed in the UV-Vis. spectra of the complexes has been studied by time-dependent DFT. The lowest 30 singlet-to-singlet spin-allowed excitation states were calculated using the same functional and basis set for the geometry optimization. In the model structures of the investigated complexes, to reduce the computer time, the phenyl ring, and two methyl groups attached to the pyrazolone ring were replaced by H atoms. The calculated d-d

excitation wave lengths, energies of other excitation transitions ($f > 0.002$) and their assignments are tabulated in Table S2†. As expected, the d-d transitions are forbidden and their oscillators' strengths are also close to 0.0. In 320-800 nm region, the stimulated spectrum of Co(II) complex showed three forbidden transitions at 761, 533 and 484 nm as well as a highest energy band at 335 nm corresponding to H(β)→L+2(β), H(β)→L+5(β), H-1(β)→L+5(β) and H(β)→ L(β), (H: HOMO, and L: LUMO). The HOMO's are mainly composed of Co d character, and LUMO orbital is of Co d_{z^2} nature (Table S3†). The transition energy at 761 nm has a ground state composed of Co d character, whereas the excitation state is of pyrazolone π^* orbitals forming a MLCT. Similar, the low oscillator strength transitions at 533 and 484 nm are MLCT to π^* system of the SO_3 groups. The band at 335 nm can be assigned to $d_{xz} \rightarrow d_{z^2}$ in an octahedral structure. The HOMO-LUMO gap in **1** is 4.22 eV, which is higher than **2**. The TD-DFT spectrum of **2** displayed three transitions at 484, 415 and 409 nm with oscillator strengths of 0.0002, 0.0017, and 0.0011, respectively. HOMO and HOMO-1 shows predominantly 3d character. HOMO-4, which is lower than HOMO by 3.65 eV, results from the π system of the pyrazolone rings (Table S4†). The two LUMO's (LUMO and LUMO+1) are lying close to HOMO with small energy gap (0.81 eV) between HOMO and LUMO. These orbitals are a mixture of π^* orbitals resulting from the two coordinated pyrazolone moieties. Hence, the electronic transitions; H-1→L (484 nm)/H→L+1 (409 nm) and H-4→ L (415 nm) are MLCT and π-π^* characters, respectively. The calculated spectrum of **3** is characterized by three lowest energy electronic transitions at 809, 569, and 526 nm assigned to H(β)→L, H-1(β)→L, and H-3(β)→L, respectively. As shown in Fig. 4, the MO's from HOMO-3 to LUMO are mainly Cu d character and energetically well separated from the next lower occupied MO's. The LUMO orbital with β-spin is mainly of Cu d_{z^2} character, whereas the HOMO orbital is coming from the Cu d_{xy}. Hence, the electronic transition at 809 nm is assigned to $d_{xz} \rightarrow d_{z^2}$ characterized to the octahedral Cu(II) complexes. The bands at 569 and 526 nm are LMCT character, originating from the pyrazolone rings and SO_3 groups and going to Cu d_{z^2}. The highest energy bands at 462, 426, and 347 nm with significant oscillator strengths are all of π-π^* character.

Natural bond orbital (NBO) analysis

According to NBO **[28]**, the electronic arrangement of Co in **1** is: $[Ar]4s^{0.20}3d^{7.56}4p^{0.41}4d^{0.01}5p^{0.01}$ with 8.167 valence electrons. The occupancies of Co 3d are: $d_{xy}{}^{1.858}\ d_{xz}{}^{0.751}\ d_{yz}{}^{1.736}\ d_{x^2-y^2}{}^{1.421}\ d_{z^2}{}^{1.794}$ .The calculated natural charge was found to be 0.821 as results of electron density donation from two tridentate molecules. Similar, the electronic configuration of Ni atom in **2** is $[Ar]4s^{0.20}3d^{8.60}4p^{0.39}5p^{0.01}$ with about one electron more in the d sub-shell (9.189) comparing with complex **1** indicating that the

quantity of the electron density donation from the two ligands is the same or slightly more excess in the Ni^{II} center. The occupancies of Ni 3d are: $d_{xy}^{1.984}$ $d_{xz}^{1.512}$ $d_{yz}^{1.919}$ $d_{x^2-y^2}^{1.326}$ $d_{z^2}^{1.857}$. For complex **3**, the electronic arrangement of Cu is $[Ar]4s^{0.24}3d^{9.33}4p^{0.37}5p^{0.01}$ distributed as 18 core electrons, 9.935 valence electrons (on 4s, 3d, and 4p atomic orbitals) and 0.010 Rydberg electrons (mainly on 5p orbital) giving total 27.945 electrons and leaving 1.053. The occupancies of Cu 3d are: $d_{xy}^{1.985}$ $d_{xz}^{1.529}$ $d_{yz}^{1.873}$ $d_{x^2-y^2}^{1.965}$ $d_{z^2}^{1.973}$. The strength of interactions between metal ion and donor sites can be estimated by the second order perturbation theory. The larger the E^2 value, the more intensive is the interaction between electron donors and electron acceptors. For complex **1**, the E^2 values are 290, 120, and 280 $calmol^{-1}$ for LP(2)O2→RY^*(2)Co/LP(2)O39→RY^*(2)Co, LP(1)N4→RY^*(2)Co/LP(1)N41→ RY^*(2)Co and LP(3)O5→RY^*(2)Co/LP(3)O43→RY^*(2)Co, in that order. These M-L interactions have energies of 230, 490, and 70 $calmol^{-1}$ in **2**, and 420, 30 and 120 $calmol^{-1}$ in complex **3**, respectively. Binding energies are defined as the total energy of complex minus the sum of total energies of the most stable isolated moieties **[29]**. Complex **2** is more stable than **1** by ≈ 2.813 $kcalmol^{-1}$, and than **3** by 22.615 $kcalmol^{-1}$. Thus, the stronger the binding capability is, the more stable the complex will be, and the higher the metal binding selectivity of a ligand to the metal ions will result. The interaction of the tertiary nitrogen with M^{n+} is the main factor determining the stability of the studied complexes, where the binding energy decreases with an increase of the M-N bond distance.

Antibacterial activity

The antimicrobial activities of analgin and its complexes were studied using two microbes; *S. aureus* and *E. coli* and compared to tetracycline used as a standard. Preliminary screening was carried out at 20 mg/mL. In classifying the antibacterial activity as Gram-positive or Gram-negative, it would be expected that a much greater number of drugs would be active against Gram-positive than Gram-negative bacteria **[30]**. Analgin showed lower activity against *S. aureus* (G^+) than tetracycline, and was inactive against *E. coli*. It is clear from the inhibition zone diameter data of the investigated complexes that the antibacterial activity of analgin is affected by type of the divalent cation. Coordination of analgin to Co(II) did not alter the toxicity, but the formation of complexes **2** and **3** results in excellent activity against the resistant *E coli* (G^-), as well as *S. aureus* bacterium. The activity of **2** and **3** did not discriminate between the tested organisms. The higher toxicity of **2** and **3** can be explained by Tweed's chelation theory **[31]**, which explicated that the lipophilicity of the free organic ligand is changed by reducing of the polarizability of the M^{n+} ion *via* the L→M donation, and the possible electron delocalization over the complexes. Lipophilicity is an important factor associated with the membrane

permeation in biological systems: the higher the lipophilicity, the easier penetration in the cell through the cellular membrane.

Conclusion

Co(II), Ni(II), and Cu(II) complexes of analgin antipyretic drug were prepared in good yields, characterized, and tested for biological activity against *S. aureus* and *E. coli*. Unequivocal proof of the tridentate nature of analgin finally came from the X-ray crystallography data. M(II) ion is arranged in a slightly distorted octahedral geometry, where two analgin molecules are acting as tridentate chelators forming four stable five-membered rings. The experimental studies were complemented by quantum chemical calculations. Coordination of analgin to Co(II) did not alter the toxicity, but the formation of Ni(II) and Cu(II) complexes results in excellent activity against the tested organisms.

Experimental

Synthesis of complexes

Instruments

FT IR spectra were recorded as potassium bromide pellets using a Jasco FTIR 460 plus in the range of 4000 to 200 cm^{-1}. Elemental microanalysis was performed using Elementer Vario EL III. TG/DTA analysis was performed in nitrogen atmosphere (20 mL min^{-1}) in a platinum crucible with a heating rate of 10 ºC min^{-1} using a Shimadzu DTG-60H simultaneous DTG/TG apparatus. Magnetic measurement was carried out on a Sherwood scientific magnetic balance using Gouy method **[30]**, and $Hg[Co(SCN)_4]$ was used as a calibrant. Electronic spectra were scanned on a Shimdazu Lambda 4B spectrophotometer in both DMSO and DMF solutions. A digital Jenway 4310 conductivity with a cell constant of 1.02 was used for the molar conductance study. X-band EPR measurements were performed on solid samples at 298 K using a Bruker EMX spectrometer. The magnetic modulation frequency was 100 kHz and the microwave power was set to 0.201 mW. The *g*-values were obtained by referencing to a diphenylpicrylhyrdazyl (DPPH) sample with $g = 2.0036$. The modulation amplitude was suited at 4 Gauss while the microwave frequency was determined as 9.775 GHz.

Synthesis

Two mmole of Analgin (646 mg) and one mmole of $Co(NO_3)_2 \cdot 6H_2O$ (291 mg), $Ni(CH_3COO)_2 \cdot 4H_2O$ (248 mg), or $Cu(NO_3)_2 \cdot 3H_2O$ (241 mg) were dissolved in ethanol (15 mL) and heated to reflux (1-3h), where pink Co(II) (**1**), blue Ni(II) (**2**) and crystalline green Cu(II) (**3**) complexes were precipitated. Diffusion of analgin solution to Cu^{2+} ions in ethanol gave green crystals suitable for X-ray structure analysis. Lower molar conductance values (in DMF) were reported for the complexes compared with

the reported values **[32]** for 1:1 (65-90 $\Omega^{-1}cm^2mol^{-1}$) and 1:2 (130-170 $\Omega^{-1}cm^2mol^{-1}$) electrolytes in DMF, indicating their non-electrolytic nature.

- Complex **1** ($C_{26}H_{32}CoN_6O_8S_2$): Yield: 73%: %Calcd. (%Found). C, 45.95 (45.48); H, 4.75 (4.77); N, 12.37 (12.63). FT IR: 1604, ν(C=O); 1331, ν(C-N); 1256 ν^{ass}(S-O); 1166 ν^{ss}(S-O); and 1019 ν^{ss}(S-O) cm^{-1}. UV-Vis. (DMF): 275 and 420 nm. μ_{eff} = 4.71 μ_B (298 K). Molar Cond. (10^{-3} M, DMF): 13.51 $\Omega^{-1}cm^2mol^{-1}$.

- Complex **2** ($C_{26}H_{32}N_6NiO_8S_2$): Yield: 77%: %Calcd. (%Found). C, 45.96 (45.39); H, 4.75 (4.78); N, 12.37 (13.50). FT IR: 1611, ν(C=O); 1331, ν(C-N); 1263 ν^{ass}(S-O); 1169 ν^{ss}(S-O); and 1022 ν^{ss}(S-O), cm^{-1}. UV-Vis. (DMF): 275, 400 and 535 nm. μ_{eff} = 3.70 μ_B (298 K). Molar Cond. (10^{-3} M, DMF): 13.01 $\Omega^{-1}cm^2mol^{-1}$.

- Complex **3** ($C_{26}H_{32}CuN_6O_8S_2$): Yield: 68%: %Calcd. (%Found). C, 45.64 (44.80); H, 4.71 (4.64); N, 12.28 (12.27). FT IR: 1600, ν(C=O); 1331, ν(C-N); 1245 ν^{ass}(S-O); 1196 ν^{ss}(S-O); and 1030 ν^{ss}(S-O), cm^{-1}. UV-Vis. (DMF): 270, 375, 485 and 780 nm. μ_{eff} = 2.57 μ_B (298 K). Molar Cond. (10^{-3} M, DMF): 18.12 $\Omega^{-1}cm^2mol^{-1}$.

X-ray diffraction analysis

Crystallographic data were collected on Enraf-Nonius CAD4 single crystal X-ray diffractometer with graphite monochromated *Mo-*K_α radiation (λ = 0.71073 Å) at 298 K. All the diffracted intensities were corrected for Lorentz-polarization and absorption [**33-34]**. The structure was solved by *SIR*92 **[35]** computer program in the space group *Pbca* and then refined with the SHELX software package **[36]**. All hydrogen atoms were included in calculated positions. The figures involving hydrogen-bonds and packing were drawn by *Mercury* **[37]**. Crystallographic data have been deposited with the Cambridge Crystallographic Data Center as supplementary publication no. CCDC-986306 for complex **3**.

DFT calculations

Geometry optimizations of complexes **1-3** in the gas phase were carried out at DFT/B3LYP method combined with LANL2DZ basis set **[38]** using Gaussian03 **[39]**, where singlet state was assigned to complex **2** and doublet state to both **1** and **3**. The starting geometry for optimization was constructed based on crystallographic data without any symmetry restriction. The complexes were characterized as local minima through harmonic frequency analysis. Electronic transitions were calculated by TD-DFT **[40]**. Natural bond orbital (NBO) analysis and the analysis frontier molecular orbitals were performed at the same level of theory.

Antibacterial activity

The antimicrobial activities of the test samples were determined by a modified *Kirby-Bauer disc diffusion method* **[41]** under standard conditions using *Mueller-Hinton* agar medium (tested for composition and pH), as described by NCCLS **[42]**. The antimicrobial activities were carried out using culture of *Staphylococcus aureus* as Gram-positive bacterium and *Escherichia coli* as Gram-negative bacterium. The solution of 20 mg/mL of each compound (free ligand, metal complexes and standard drug *Tetracycline*) in DMSO was prepared for testing. Centrifuged pellets of bacteria from a 24 h old culture containing approximately 10^4-10^6 CFU/mL (colony forming unit) were spread on the surface of *Mueller Hinton* Agar plates. Then the wells were seeded with 10 mL of prepared inocula to have 10^6 CFU/ml. Petri plates were prepared by pouring 100 mL of seeded nutrient agar. DMSO (0.1 mL) alone was used as control under the same conditions for each microorganism, subtracting the diameter of inhibition zone resulting with DMSO, from that obtained in each case. The antimicrobial activities could be calculated as a mean of three replicates.

Acknowledgment

I thank Dr: Krzysztof Radacki, Julius-Maximilians-Universität Würzburg, Germany, for refining the crystal structure of compound 3.

References:

[1] **(a)** A. Korolkovas, J.H. Burckhalter, Química Farmacêutica, Guanabara Koogan, Rio de Janeiro, 1988, pp. 193-195, **(b)** R.N. Brogden, Drugs 32 (Suppl. 4) (1986) 60-70, **(c)** A. Wong, A. Sibbald, F. Ferrero, M. Plager, M.E. Santolaya, A.M. Escobar, S. Campos, S. Barragan, M. De Leon Gonzalez, G.L. Kesselring, Clin. Pediatr. (Phil.) 40 (2001) 313-324.

[2] H. Ergun, I.H. Ayhan, F.C. Tulunay, Gen. Pharmacol. 33 (1999) 237-241.

[3] C. Muriel-Villoria, E. Zungri-Telo, M. Diaz-Curiel, M. Fernandez-Guerrero, J. Moreno, J. Puerta, P. Ortiz, Eur. J. Clin. Pharmacol. 48 (1995) 103-107.

[4] Martindale, The Complete Drug Reference, 32nd ed., Pharmaceutical Press, London, 1999.

[5] E. Zylber-Katz, L. Granit, M. Levy, Eur. J. Clin. Pharmacol. 42 (1992) 187-191.

[6] **(a)** S.Z. Qureshi, A. Saeed, T. Hasan, Talanta 36(8) (1989) 869-871, (b) N.V. Pathak and I.C. Shukla, J. Indian Chem. Soc. 60, 206-207 (1983).

[7] T. Perez-Ruiz, C. Martinez-Lozano, V. Tomas, J. Carpena, Microchem. J. 47 (1993) 296-301.

[8] N.H. Eddine, F. Bressolle, B. Mandrou, H. Fabre, Analyst 107, 67-70 (1982).

[9] **(a)** T. Pkrez-Ruiz, C. Martinez-Lozano, V. Tomas, J. Pharm. Biomed. Anal. 12(9), (1994) 1109-1113, **(b)** L.H. Marcolino-Júnior, M.F. Bergamini, M.F.S. Teixeira, E.T.G. Cavalheiro, O. Fatibello -Filho, IL Farmaco 58 (2003) 999-1004.

[10] F. Belal, Electroanalysis 4 (1992) 589.

[11] F. Marchetti, C. Pettinari, R. Pettinari, Coordination Chemistry Reviews 249 (2005) 2909-2945.

[12] J.S. Casas, M.S. García-Tasende, A. Sánchez, J. Sordo, A. Touceda, Coord. Chem. Rev. 251 (11-12) (2007) 1561-1589.

[13] S.V. Tatwawadi, A.P. Singh, K.K. Narang, Indian J. Chem., Section A: Inorg. Phy. Theo. & Anal. (1982), 21A(6), 644-5.

[14] **(a)** R.C. Maurya, S. Rajput, Synthesis and Reactivity in Inorganic and Metal-Organic Chemistry (2003), 33(10), 1877-1894, **(b)** R.C. Maurya, N. Chturvedi, S.K. Thakur, Journal of the Institution of Chemists (1999), 71(6), 216-220, **(c)** R.C. Maurya, V. Pillai, S. Rajput, Synthesis and Reactivity in Inorganic and Metal-Organic Chemistry (2003), 33(4), 699-716, **(d)** R.C. Maurya, D.K. Shrivastava, T. Singh, Journal of the Institution of Chemists (1999), 71(5), 198-201, **(e)** R.C. Maurya, D.D. Mishra, Synthesis and Reactivity in Inorganic and Metal-Organic Chemistry (1988), 18(2), 133-40, **(f)** R.C. Maurya, R. Verma, B. Shukla, Indian Journal of Chemistry, Section A: Inorganic, Bio-inorganic, Physical, Theoretical & Analytical Chemistry (1999), 38A(7), 730-735, **(g)** R.C. Maurya, J. Dubey, B. Shukla, Synthesis and Reactivity in Inorganic and Metal-Organic Chemistry (1998), 28(7), 1159-1171, **(h)** R.C. Maurya, D.D. Mishra, P.K. Trivedi, A. Gupta, Synthesis and Reactivity in Inorganic and Metal-Organic Chemistry (1994), 24(1), 17-28, **(i)** R.C. Maurya, D.D. Mishra, S. Pillai, Synthesis and Reactivity in Inorganic and Metal-Organic Chemistry (1997), 27(10), 1453-1466, **(j)** R.C. Maurya, D.D. Mishra, V. Pillai, Synthesis and Reactivity in Inorganic and Metal-Organic Chemistry (1995), 25(7), 1127-41, **(k)** R.C. Maurya, D.D. Mishra, V. Pillai, Synthesis and Reactivity in Inorganic and Metal-Organic Chemistry (1995), 25(1), 139-50, **(l)** R.C. Maurya, D.D. Mishra, S. Mukherjee, P.K. Trivedi, Transition Metal Chemistry (Dordrecht, Netherlands) (1991), 16(5), 524-7.

[15] N.N. Shaforostova, N.A. Skorik, E.N. Naprienko, Zhurnal Neorganicheskoi Khimii (2000), 45(8), 1344-1349.

[16] O.A. Gabrichidze, Koordinatsionnaya Khimiya (1988), 14(12), 1632-5.

[17] M.G. Miles, G. Doyle, R.P. Cooney, R.S. Tobias, Spectrochim. Acta 25A (1969) 1515-1526.

[18] T.B. Chenskaya, M. Berghahn, P.C. Kunz, W. Frank, W. Kläui, J. Mol. Struct. 829 (2007) 135-148.

[19] M.V. Marinho, L.F. Marques, R. Diniz, H.O. Stumpf, L.C. Visentin, M.I. Yoshida, F.C. Machado , F. Lioret, M. Julve, Polyhedron 45 (2012) 1-8.

[20] A.B.P. Lever; "Inorganic Electronic Spectroscopy", 2nd Edition, Elsevier, Amsterdam, (1982).

[21] A. Cotton, G. Wilkinson, advanced Inorganic Chemistry, 2nd Ed. 1972.

[22] E. González, A. Rodrigue-Witchel, C. Reber, Coord. Chem. Rev. 251 (2007) 351-363.

[23] A. Seminara, A. Musumeci, R.P. Bonomo, Inorg. Chim. Acta 90 (1984) 9-15.

[24] N.T. Abdel-Ghani, M.F. Abo El-Ghar, A.M. Mansour, Spectrochim. Acta A 104 (2013) 134-142.

[25] J.A. Welleman, F.B. Hulsbergen, J. Verbiest, J. Reddijk, J. Inorg. Nucl. Chem. 40 (1978) 143-147.

[26] R.J. Rudley, B.J. Hathaway, J. Chem. Soc. (1970) 1725-1728.

[27] B.J. Hathaway, D.E. Billing, Coord. Chem. Rev. 5 (1970) 143-207.

[28] (a) A.E. Reed, L.A. Curtiuss, F. Weinhold, Chem. Rev. 88 (1988) 899, **(b)** A.M. Mansour, Inorg. Chim. Acta 408 (2013) 186-192.

[29] A.M. Mansour, Inorg. Chim. Acta 394 (2013) 436-445.

[30] A.M. Mansour, Spectrochim. Acta A 123 (2014) 257-266.

[31] B. Tweedy; Phytopathalogy 55 (1964) 910.

[32] J. Pons, A. Chadghan, J. Casabó, A. Alvarez-Larena, J. Francesc Piniella, J. Ros; Polyhedron 20 (2001) 2531.

[33] A.L. Spek; J. Appl. Cryst., 36 (2003) 7-13.

[34] A.L. Spek; Program for reduction of CAD-4 Data, University of Utrecht, The Netherlands, 1996.

[35] A. Altomare, G. Cascarano, C. Giacovazzo, A. Guagliardi, M. C. Burla, G. Polidori, M. Camalli; J. Appl. Cryst., 27 (1994) 435-436.

[36] G. M. Sheldrick, Acta Crystallogr., Sect. A: Fundam. Crystallogr., 2008, 64, 112.

[37] C. K. Johnson, 1976. ORTEP--II. A Fortran Thermal--Ellipsoid Plot Program. Report ORNL-5138. Oak Ridge National Laboratory, Oak Ridge, Tennessee, USA.

[38] A.M. Mansour, Polyhedron, 78 (2014) 10-17.

[39] M.J. Frisch, G.W. Trucks, H.B. Schlegel, G.E. Scuseria, M.A. Robb, J.R. Cheeseman, V.G. Zakrzewski, J.A. Montgomery, R.E. Stratmann, J.C. Burant, S. Dapprich, J.M. Millam, A.D. Daniels, K.N. Kudin, M.C. Strain, O. Farkas, J. Tomasi, V. Barone, M. Cossi, R. Cammi, B. Mennucci, C. Pomelli, C. Adamo, S. Clifford, J. Ochterski, G.A. Petersson, P.Y. Ayala, Q. Cui, K. Morokuma, D.K. Malick, A.D. Rabuck, K. Raghavachari, J.B. Foresman, J. Cioslowski, J.V. Ortiz, A.G. Baboul, B.B. Stefanov, G. Liu, A. Liashenko, P. Piskorz, I. Komaromi, R. Gomperts, R.L. Martin, D.J. Fox, T. Keith, M.A. Al-Laham, C.Y. Peng, A. Nanayakkara, C. Gonzalez, M. Challacombe, P.M.W. Gill, B. G. Johnson, W. Chen, M.W. Wong, J.L. Andres, M. Head-Gordon, E.S. Replogle, J.A. Pople, GAUSSIAN 03 (Revision A.9), Gaussian, Inc., Pittsburgh, (2003).

[40] N.T. Abdel-Ghani, A.M. Mansour, J. Coord. Chem. 65(5) (2012) 763-779.

[41] N.T. Abdel-Ghani, A.M. Mansour; Eur. J. Med. Chem. 47 (2012) 399.

[42] National Committee for Clinical Laboratory Standards, NCCLS Approval Standard Document M2-A7, Vilanova, PA, (2000).

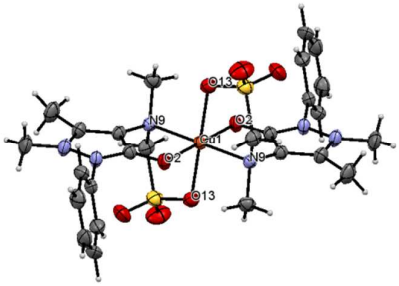

Coordination of analgin to Ni(II) and Cu(II) ions as a mono-negatively tridentate ligand leads to a significant increase in its antibacterial activity compared with the Co(II) complex.